



Evolution of adsorption isotherm and isosteric heat from sub-triple to super-critical points

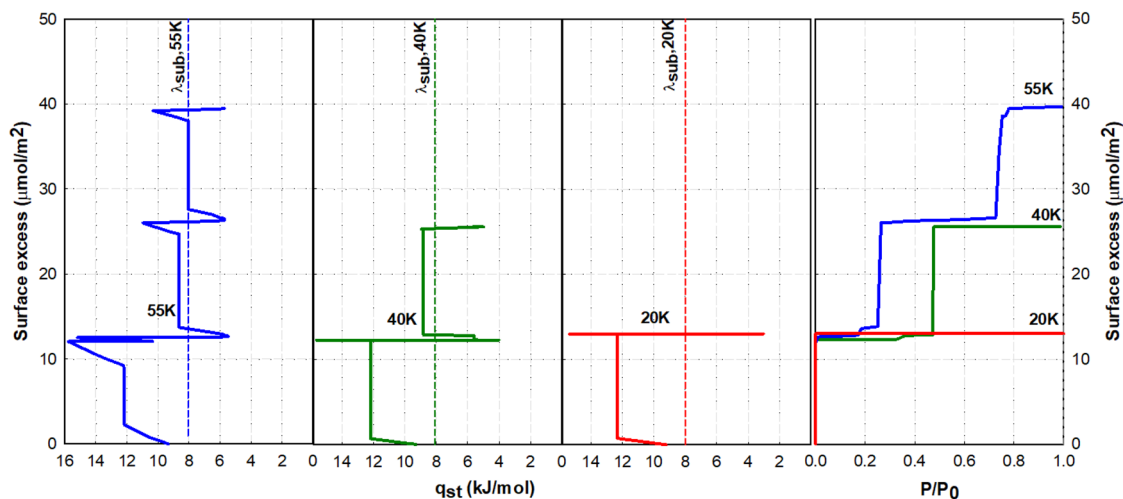
Luis Herrera¹ · Quang K. Loi² · Luisa Prasetyo² · D. D. Do²

Received: 18 August 2020 / Revised: 8 November 2020 / Accepted: 20 December 2020 / Published online: 25 January 2021
© The Author(s), under exclusive licence to Springer Science+Business Media, LLC part of Springer Nature 2021

Abstract

We carried out a comprehensive molecular simulation to investigate the evolution of the excess isotherms and the isosteric heat with respect to temperature for argon adsorption on strong and weak substrates. The temperature ranges from well below the bulk triple point temperature to above the bulk critical temperature to show the first- (second-) order transitions and the state of the system at the bulk coexistence pressure P_0 , whether it is non-wetting, partial wetting or complete wetting (preceded by pre-wetting). It is found that the key parameter that affects the dependence of the transitions on temperature and the state of the system at P_0 is the relative difference between the isosteric heat and the heat of sublimation (or condensation). For strong substrates, the state of the system changes from partial wetting to complete wetting when the temperature crosses the bulk triple point temperature, and for temperatures well below the bulk triple point the 2D-condensation occurs in the first and second (and possible higher) layers. For weak substrates, the state of the system changes from non-wetting to complete wetting when the temperature crosses the wetting temperature T_w , which is specific to the substrate. For temperatures greater than T_w , complete wetting in weak substrates only occurs at pressures close to the bulk coexistence pressure P_0 via the initial stage of clustering (unfavourable adsorption), followed by a pre-wetting (known as thin-to-thick transition), and this is reflected in the increase of the isosteric heat from a value less than the heat of condensation λ and approaching λ as the pressure tends to P_0 .

Graphic abstract



Keywords Excess isotherm · Isosteric heat · Wetting · Pre-wetting · Partial wetting

Contribution to a special issue in honour of Shijavi Sircar.

Extended author information available on the last page of the article

1 Introduction

Adsorption has been a subject of interest in the literature of adsorption science and engineering since the first report by Kayser in 1881 Robens and Jayaweera [1]. In the past many decades, adsorption has diversified and evolved rapidly with many potential applications in chemical and biochemical industries. Parallel to researches in adsorption science are those in colloid sciences with different terminologies used in those disciplines, for example, molecular layering/clustering, and non-wetting/partial wetting/pre-wetting/wetting. Despite the different choice of terms, the common denominator is the potential energy of interaction between various entities in a system. Recent work shows the correlation between molecular layering and clustering and the observed phenomenon of either non-wetting/pre-wetting/wetting when the pressure of the bulk surrounding has reached the coexistence pressure of the bulk phase [2–4]. These studies are relevant in many applications such as environmental science, petroleum engineering and biomedical applications [5–8], for which the transition between non-wetting to wetting could affect the performance of a system. We have found that the important parameters that affect the transition are the affinity of the surface and temperature [9–12]. In this work, we show how the excess isotherm and the isosteric heat on a flat and open surface, which are important in the assessment of the performance of the adsorbate/adsorbent pair [13–18], would evolve with respect to temperature for a wide range of temperature spanning from those well below the bulk triple point temperature to those well above the bulk critical point temperature [10, 11, 19]. The same concept can be extended to adsorption in pores (e.g. slit pore) which is complicated by the enhancement in the adsorbate–adsorbent potential and the confinement of the system but is not the focus of this study.

Specifically, the fundamental factors that govern the transition between non-wetting/pre-wetting and wetting on flat and open surfaces are:

- the intermolecular interactions between adsorbate molecules,
- the interactions between adsorbate and solid adsorbent, and
- the temperature.

Figure 1 shows the wetting map of argon on a flat and open surface that demarcates regions of non-wetting/partial wetting/pre-wetting and complete wetting at the bulk coexistence pressure as a function of the temperature and the affinity of the solid substrate [10, 19]. The affinity is described by the parameter D^* , which is the ratio of the minimum of the energy interaction between a fluid particle

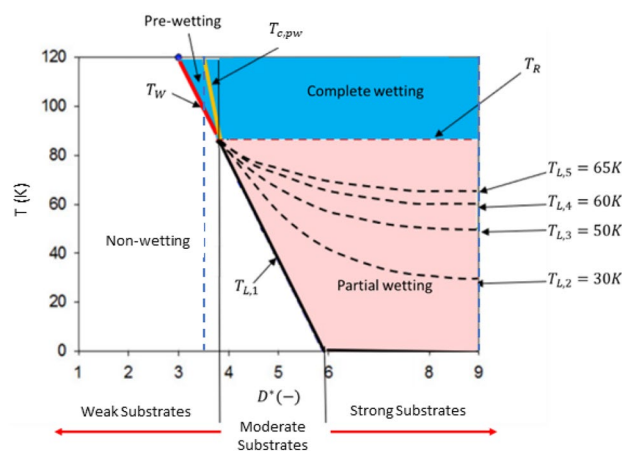


Fig. 1 Wetting diagram of argon on a flat and open surface, demarcating the regions of non-wetting, partial wetting and complete wetting. The two vertical dashed blue lines mark the D^* values of 3.5 and 9.0 for the substrates studied in this paper

and the solid ($|\varphi_{sf}|$) to the minimum of the fluid–fluid potential energy ($|\varphi_{ff}|$).

$$D^* = \left| \frac{\varphi_{sf}}{\varphi_{ff}} \right| \quad (1)$$

The four distinct regions in the wetting map are:

- Non-wetting region: This is observed for weak substrates, and it is identified with the finite adsorbed density (typically less than one statistical monolayer density) at the bulk coexistence pressure P_0 , and the adsorption isotherm crosses the P_0 axis at a finite angle.
- Partial wetting region: This region is commonly observed with moderate and strong substrates, and it is demarcated by the layering temperature of the first layer, $T_{L,1}$, which is defined as the temperature at which the monolayer is formed at P_0 , and the roughening temperature T_R , which is defined as the temperature at which the interface between the adsorbed film and the bulk gas is sufficiently undulated such that complete wetting occurs at P_0 . For temperatures falling between $T_{L,1}$ and T_R , this partial wetting region is sub-divided into many sub-regions, demarcated by the temperature $T_{L,k}$, which is the temperature at which the layer k is formed at P_0 ; for example in the sub-region demarcated by $T_{L,k}$ and $T_{L,k+1}$ only k layers are formed at P_0 .
- Complete wetting region: This is the region for temperatures either greater than the roughening temperature or the critical pre-wetting temperature. Complete wetting occurs at P_0 as identified by the adsorbed density approaching infinity as the pressure tends to P_0 .

- **Pre-wetting region:** This region is very narrow and falls between the non-wetting region and the complete wetting region. It is demarcated between the wetting temperature T_W (the red line) and the critical pre-wetting temperature $T_{c,pw}$ (yellow line). It is important to make a distinction between T_W and $T_{L,1}$ in Fig. 1 with the former being the one that the complete wetting occurs at P_0 while the latter is one at which only a monolayer is formed at P_0 . This pre-wetting region is known in the literature as the thin-to-thick film transition region. Its name is chosen to reflect the sharp increase in the adsorbed density from a typically much lower than the statistical monolayer density V_m , to a density which is a multiple of V_m . This pre-wetting transition occurs at a pressure close to P_0 . The sharp increase in density has been explained as the transition from the agglomeration of clusters to form a molecular film of many layers [10, 19].

2 Theory

2.1 Simulation methods

Monte Carlo simulations were carried out with two-volume canonical ensemble [20, 21] and Grand Canonical ensemble to obtain the isotherm and the isosteric heat for argon adsorption on solid substrates of different strength over a range of temperatures from those below the bulk triple point temperature to above the bulk critical temperature.

2.1.1 Volumetric method (2V-NVT)

The two-volume canonical ensemble was used to determine the isosteric heat of adsorption across the first-order transition, which is not possible with the grand canonical simulation. This method involves two simulation boxes: the adsorption volume and the bulk gas volume. Two types of move are used: the displacement of a molecule and the exchange of a molecule between the two boxes, 150,000 cycles were used in the equilibration, and sampling stages with each cycle consisting of 1000 trial moves with 50/50 probability for the displacement and exchange moves [10]. The maximum displacement length was initially set as 2 nm and adjusted at the end of each cycle of the equilibration stage to give an acceptance ratio of 20%, and it was then kept constant in the sampling stage.

2.1.2 Grand canonical Monte Carlo (GCMC)

In simulations with grand canonical ensembles, 150,000 cycles are also used in the equilibration and sampling stages,

and each cycle has 1000 trial moves of displacement, insertion and deletion with equal probability. We adjust the displacement length in the equilibration stage the same way as in the two-volume canonical simulation. The Johnson et al.’s equation of state [22] is used to calculate the chemical potential for each pressure used in the simulation.

2.1.3 Solid–fluid (S.F.) and fluid–fluid (F.F.) potentials

The intermolecular energy of interaction of argon is calculated with the Lennard–Jones 12–6 equation with molecular parameters $\sigma_{ff} = 0.3405$ nm and $\epsilon_{ff} = 119.8$ K [23]. The interaction energy between an argon molecule and the solid substrate is calculated with the 10–4–3 equation [24]. Here we modelled the solid substrate as a composite of planar layers of constant surface density and equally spaced.

$$\varphi_s = 2\pi\rho_s\epsilon_{sf}\sigma_{sf}^2 \left[\frac{2}{5} \left(\frac{\sigma_{sf}}{z} \right)^{10} - \left(\frac{\sigma_{sf}}{z} \right)^4 - \frac{(\sigma_{sf})^4}{3\Delta(0.61\Delta + z)^3} \right] \tag{2}$$

where z is the shortest distance between the centre of argon molecule and the surface. The interspacing between layers Δ is 0.3354 nm, and a surface density ρ_s is 38.2 nm^{-2} . The cross molecular parameters are calculated with the Lorentz–Berthelot mixing rules. To model the different strength of the solid substrate, we varied the well depth of the interaction energy ϵ_{ss}/k_B (k_B is the Boltzmann constant) for the solid atom. For a strong substrate, we chose graphite with the collision diameter and well-depth for a carbon atom in a graphene layer, σ_{ss} of 0.34 nm and $\epsilon_{ss}/k_B = 28$ K, while for the weak substrate we chose the same collision diameter for the solid atom and $\epsilon_{ss}/k_B = 4.2$ K. The corresponding D^* for the strong and weak substrates are 9 and 3.5, respectively.

2.2 Thermodynamic properties

2.2.1 Surface excess

Adsorption isotherms are obtained as plots of the excess density versus pressure for a range of temperatures tabulated in Table 1. The excess density is calculated from

$$\Gamma_{ex} = \frac{\langle N \rangle - V_{acc}\rho_G}{L_x L_y} \tag{3}$$

where $\langle N \rangle$ is the ensemble-average number of molecules in the simulation box and V_{acc} is the accessible volume [25], ρ_G is the bulk gas density and $L_x L_y$ is the area of the solid substrate. The accessible volume is defined as the volume within which the interaction energy between a molecule and the solid substrate is non-positive.

Table 1 The temperatures used in this work and their corresponding coexistence pressures of the bulk phase

T (K)	P_0 (Pa)
20	6.15×10^{-12}
40	2.14×10^{-1}
55	1.52×10^2
65	2.23×10^3
87	8.83×10^4
110	6.10×10^5
150	4.37×10^6

To compare the isotherms at temperatures below the bulk critical temperature, we also plotted the isotherm in terms of the reduced pressure P/P_0 , where P_0 is the coexistence pressure of the bulk. For the proper assessment of this comparison, the pressure P_0 must be calculated correctly. For temperatures below the bulk triple point temperature, it is calculated with the simulated correlation results obtained from the vapour-solid equilibria of Chen, Siepmann and Klein [26], while for temperatures above the bulk triple point temperature and less than the bulk critical point temperature we obtained P_0 from the simulation of vapor-liquid equilibria (VLE) [27]. The values for P_0 at various temperatures used in this work are tabulated in Table 1.

2.2.2 Isosteric heat

The isosteric heats of adsorption q_{st} is obtained in the grand canonical simulation with the fluctuation theory. It is given in Eq. 4, and it accounts for the nonideality of the bulk gas [28].

$$q_{st} = \frac{N_G}{f(N_G, N_G)} kT - \frac{f(U, N)}{f(N, N) - f(N_G, N_G)} \quad (4)$$

where U is the potential energy and N is the number of molecules in the system, and N_G is the number of molecules occupying the accessible volume at the same density as the bulk gas surrounding, and the fluctuation variable f is given by

$$f(X, Y) = \langle XY \rangle - \langle X \rangle \langle Y \rangle \quad (5)$$

with $\langle \cdot \rangle$ being the ensemble average.

2.2.3 Local density distribution

The local density distribution of molecules as a function of distance above the substrate surface is calculated from

$$\rho(z) = \frac{\langle \Delta N_{z, z+\Delta z} \rangle}{L_x L_y \Delta z} \quad (6)$$

where $\langle \Delta N_{z, z+\Delta z} \rangle$ is the ensemble-average of the number of molecules whose centres of mass are between z and $z + \Delta z$.

3 Results and discussion

3.1 Strong adsorbing substrate (graphite)

3.1.1 Adsorption isotherm

- Temperatures below the bulk triple point temperature.

We started with graphite ($D^* = 9$), representing strong substrate, and the adsorption isotherms at various temperatures are shown in Fig. 2 as plots of the excess density versus pressure and also versus reduced pressure. Below the bulk triple point, we used 20 K, 40 K and 55 K as representative temperatures to show the extent of the partial wetting. According to the wetting map of Fig. 1, there is one layer for 20 K, two layers for 40 K and three layers for 55 K formed on the surface at P_0 . Their isotherms intersect the P_0 axis at a practically 90-degree angle, typical of the layer-by-layer (stepwise) mechanism of adsorption. This is called the partial wetting because the adsorbed film is finite in thickness at P_0 .

Similar to the 20 K-isotherm, the isotherm at 40 K in Fig. 2 exhibits a partial wetting behaviour, but there are two layers formed on graphite at P_0 . This is because this temperature is between the layering temperatures of the second and third layers, $T_{L,2} = 30$ K and $T_{L,3} = 50$ K.

As the final example of partial wetting, we considered 55 K-isotherm that shows three layers on the surface of graphite at P_0 . When we considered the behaviour of the 20 K-, 40 K- and 55 K-isotherms plotted in terms of the reduced pressure, it is seen that the first-order transition for the condensation of the first layer occurs at higher reduced pressure with temperature. This is due to the greater isosteric heat of adsorption at zero loading than the heat of sublimation of the bulk phase. However, when we considered the first-order transition for the formation of the second layer for the cases of 40 K- and 55 K-isotherms, we observed the opposite, i.e. it occurs at the lower reduced pressure for higher temperature (55 K). This is simply due to the fact that the isosteric heat of adsorption at the point just prior to the condensation of the second layer is less than the heat of sublimation. We shall discuss this in greater details in Sect. 3.1.3.

- Temperatures between the bulk triple point and critical point temperatures.

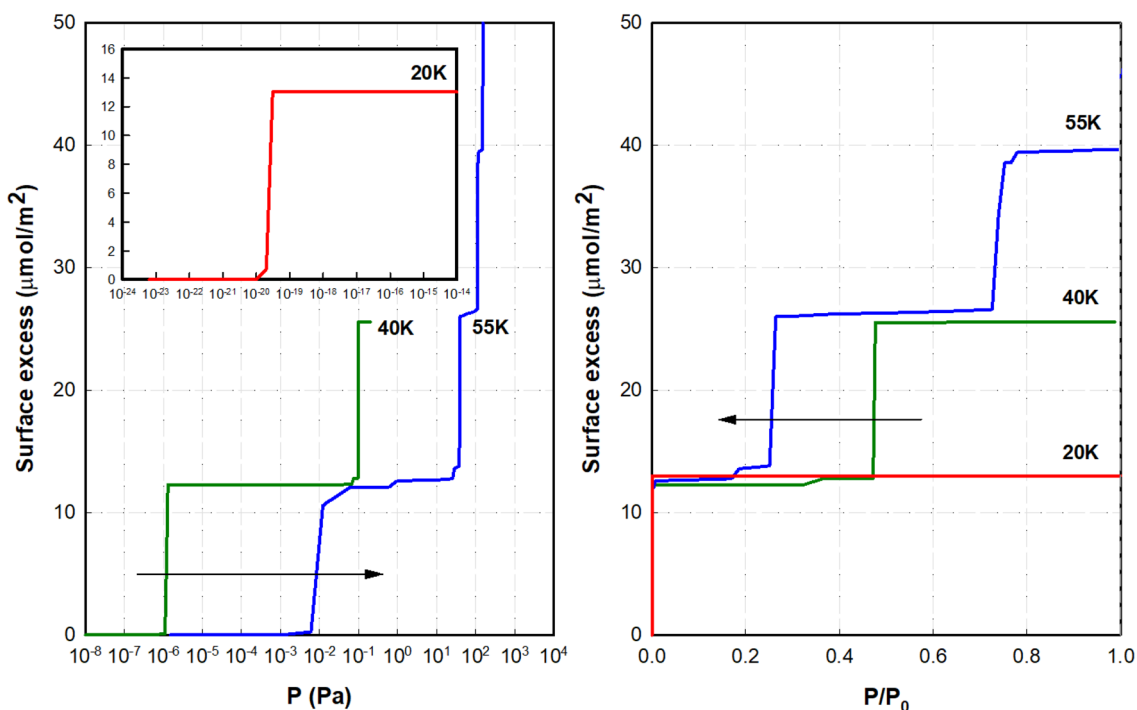


Fig. 2 Isotherms for argon adsorption on graphite at 20 K, 40 K and 55 K, plotted in terms of the absolute pressure (left panel) and the reduced pressure P/P_0 (right panel), where P_0 is given in Table 1. Note the extremely low pressure for the onset of condensation of the first layer at 20 K

We took 87 K and 110 K as examples to illustrate the adsorption behaviour for the temperature range between the triple point and critical temperatures of the bulk. These temperatures are above the roughening temperature 83.8K (which is the same as the bulk triple point temperature), and as a result, the adsorbed density tends to infinity as the pressure approaches the bulk coexistence pressure P_0 . This is complete wetting, which is the case for all temperatures falling between the bulk triple and critical temperatures. Instead of exhibiting stepwise behaviour as displayed for temperatures below the bulk triple point temperature, the 87 K- and 110 K-isotherms exhibit a monotonic behaviour of type II, according to the IUPAC classification, i.e. higher molecular layers are progressively formed before the lower layers are completely formed. When plotted against the reduced pressure, we see that at a given reduced pressure the adsorbed density is greater for lower temperature, and this is due to the higher local density that results in stronger adsorbate–adsorbate interactions for greater adsorption (Fig. 3).

- Temperatures above the bulk critical point temperature

We took 200 K and 253 K as examples to illustrate the behaviour of the excess isotherm for temperatures greater than the bulk critical point temperature. These excess isotherms exhibit a different pattern than those below the critical point, in that, they show a maximum at which the change

of the density in the system is the same as the change of the bulk density with respect to a differential change in pressure. Beyond this maximum, the excess density decreases with pressure, but it remains positive because we used the accessible volume in the calculation of the excess density [25]. An overestimation of the pore volume can result in negative excess adsorption amounts [29].

We also presented in Fig. 4 the isotherms at 150 K, just before the bulk critical point, and 160 K, just after the bulk critical point to show the interesting behaviour near the critical point. The 150 K-isotherm exhibits a wetting behaviour, similar to what has been discussed for 87 K and 110 K earlier, while the 160 K-isotherm initially behaves like a sub-critical vapour, but as the critical pressure is reached the isotherm exhibits a sharp maximum, beyond which the adsorbed density decreases very sharply, and this is simply due to the significant change in the bulk density for a small change in pressure in the neighbourhood of the critical point. A detailed discussion of isotherms in the neighbourhood of the critical point has been reported in the literature [30, 31].

3.1.2 Local density distribution

- Temperatures below the bulk triple point temperature

Fig. 3 Isotherms for argon adsorption on graphite at 87 K and 110 K, plotted in terms of the absolute pressure (left panel) and the reduced pressure P/P_0 (right panel), where P_0 is given in Table 1

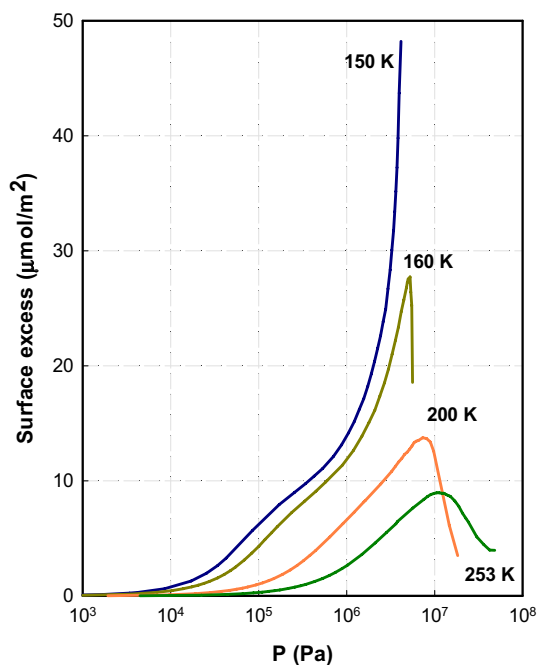
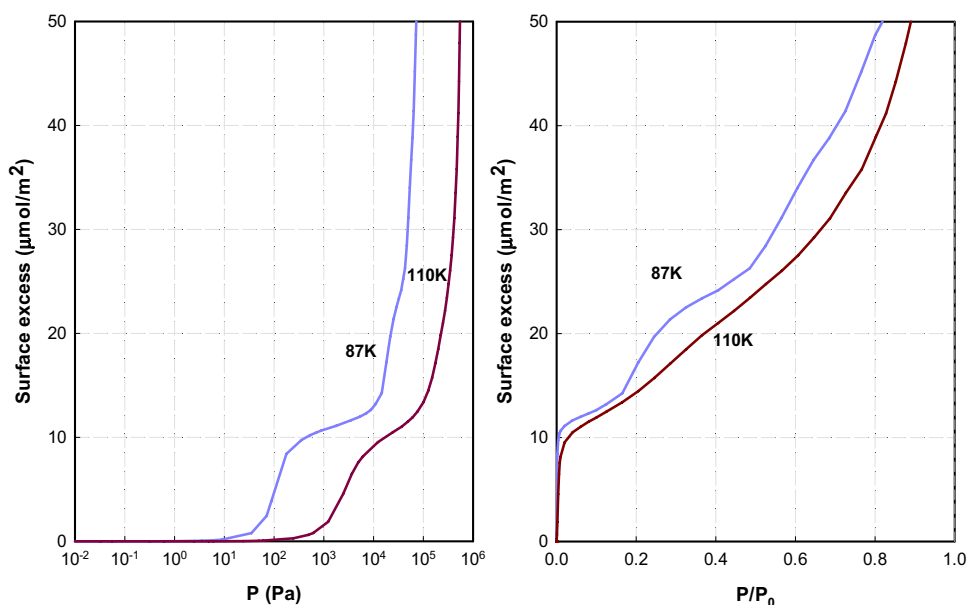


Fig. 4 Isotherms for argon adsorption on graphite at 150 K, 160 K, 200 K and 253 K plotted in terms of absolute pressure

To substantiate the behaviour of isotherms discussed in Sect. 3.1.1, we presented in Fig. 5 the local density distributions (LDDs) at 20 K, 40 K and 55 K and at their respective coexistence pressures.

This figure confirms the formation of a single layer at 20 K, two layers at 40 K and up to three layers at 55 K. It also shows the effects of the thermal fluctuations that make the

peak broader at high temperatures, i.e. molecules vibrate vertically from the equilibrium positions with larger amplitude at a higher temperature. Because of the broader peak, its height is lower as seen in the comparison between the first peaks for 20 K and 55 K (see top figure), resulted from the fact that the area under the peak is the number of molecules for a complete monolayer (which is constant).

- Temperatures between the bulk triple point and critical point temperatures

Figure 6 shows the LDDs at P_0 for 87 K and 110 K, which shows the complete wetting behaviour with a large number of molecular layers on graphite. The LDDs show an oscillating behaviour, indicating the molecular layer structure of the adsorbed film, and as the loading is increased the local density at distances far away from the surface is essentially the same as the bulk liquid density. This is because the interface of the thick adsorbed film is undulated to the extent that incoming molecules to the adsorbed film as if it were in the bulk liquid phase, resulting in the isosteric heat equalling the heat of condensation. We shall substantiate this with the analysis of the isosteric heat as a function of loading in Sect. 3.1.3.

The effects of temperature are also seen with these LDDs that the peaks are broader and lower in height for high temperatures, resulting from the greater vibration from the equilibrium position. For this same reason, the interspacing between peaks is also slightly greater with temperature.

- Temperatures above the bulk critical point temperature

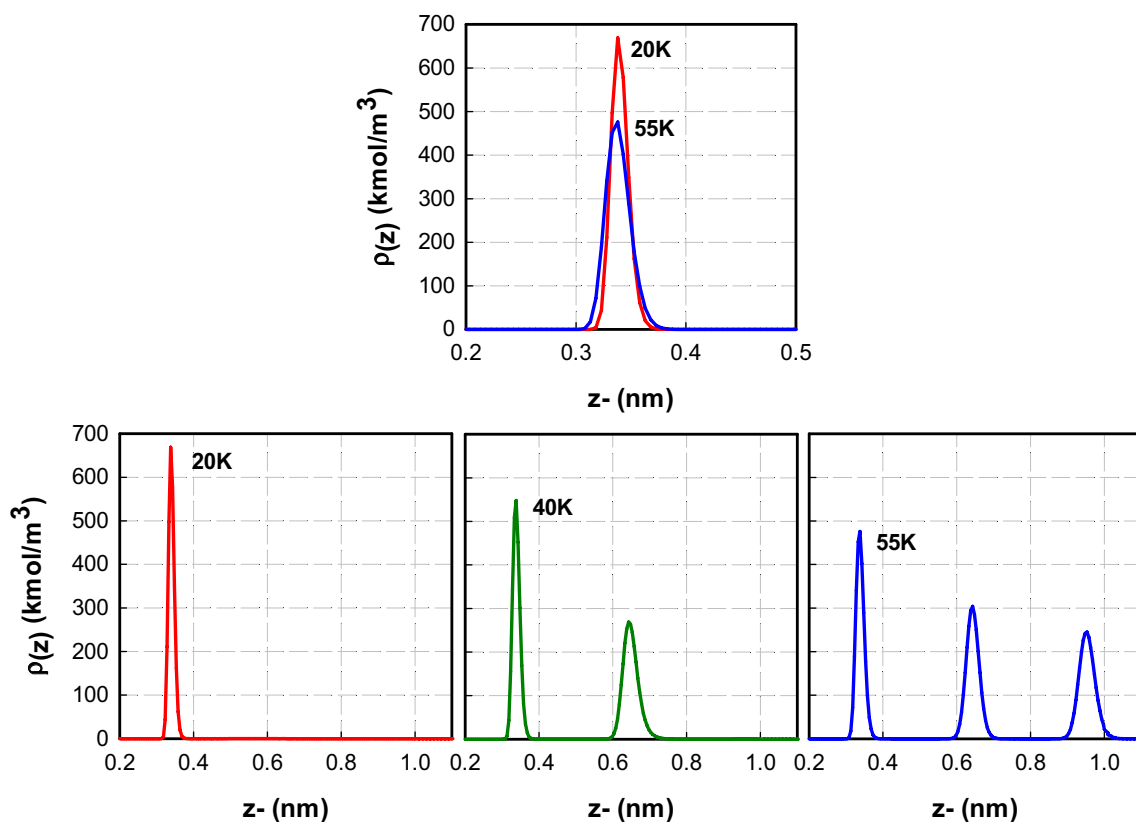


Fig. 5 Local density distributions (LDDs) for argon adsorption on graphite at 20 K, 40 K and 55 K at their respective coexistence pressures P_0 , tabulated in Table 1

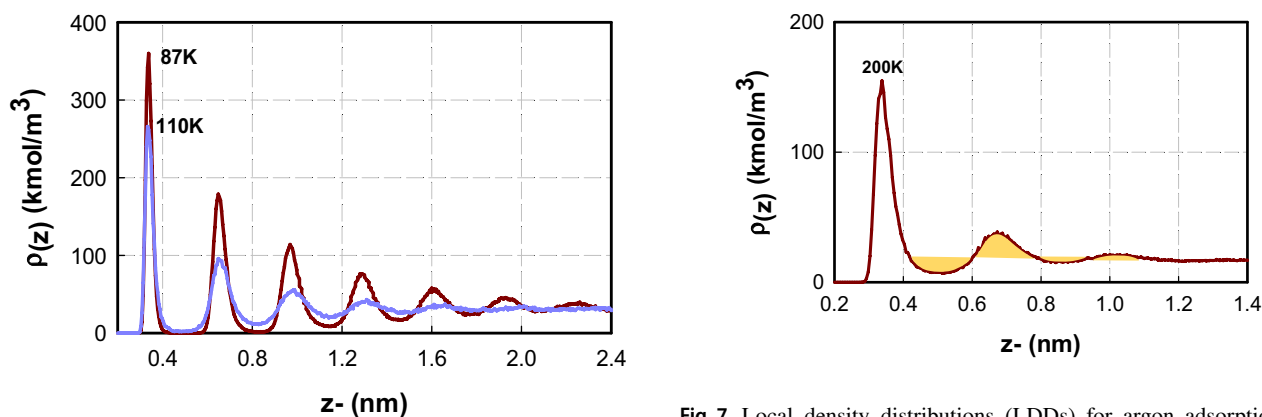


Fig. 6 Local density distributions (LDDs) for argon adsorption on graphite at 87 K (red) and 110 K (blue) at their respective coexistence pressures P_0 , tabulated in Table 1

Fig. 7 Local density distributions (LDDs) for argon adsorption on graphite at 200 K and 1.62×10^7 Pa

Figure 7 shows the LDDs for temperatures above the critical temperature. Although they show alternate peaks and troughs, it does not mean that many dense layers are formed on the surface, but rather the high local densities of the peaks for the second and higher layers cancel out the low local densities in the corresponding troughs (see yellow

regions in the figure). Macroscopically speaking, this is not regarded as molecular layering as seen for temperatures less than the bulk critical point temperature (Fig. 6), but rather it is the densification of adsorbate. It is the presence of the surface of strong affinity that gives rise to the excess equivalent to one statistical monolayer [32].

3.1.3 Isothermic heat as a function of loading

To understand how the excess isotherm behaves with pressure and temperature, we studied the isosteric heat of adsorption as a function of loading, as presented in Figs. 8, 10 and 11 for temperatures below the triple point temperatures, for temperatures between the triple point and critical temperatures, and temperatures above the critical temperature, respectively. These isosteric heats are compared with the heat of sublimation or the heat of condensation to show the competition between the adhesive force in adsorption and the cohesive for the bulk phase.

- Temperatures below the bulk triple point temperature

Take 20 K as the first example; the isosteric heat of adsorption at zero loading is 9.5 kJ/mol, which is greater than the bulk heat of sublimation of 8 kJ/mol (Fig. 8), suggesting that adsorption is favourable in that molecules initially adsorb on the surface as clusters because of the low entropic factor. These clusters coalesce to form islands with loading, and as further molecules are added, they adsorb at the boundary of these islands [33]. It is this boundary growth that incoming molecules interact with three nearest neighbouring molecules, resulting in a constant heat of adsorption (12.3 kJ/mol) across this first-order transition of condensation to form the first layer. After the condensation has been completed, further molecules are added to densify the first layer for which the adsorbed molecules form a hexagonal packing, at which the isosteric heat reaches a maximum of 15.4 kJ/mol. This maximum is achieved because of the optimal spacing between adsorbed molecules, i.e. each molecule

interacts six nearest molecules at a spacing very close to $2^{1/6}\sigma_{ff}$, the optimal spacing of a pair of molecules (Fig. 9).

We substantiated the maximum isosteric heat of adsorption at the completion of the first layer by studying the energetic of molecules when the first layer is completely formed. A molecule is randomly selected from a configuration of this monolayer and moved vertically from the surface, and its energies of interaction with the remaining molecules and graphite are calculated, and they are presented in Fig. 9 as a function of distance from the surface; the black line is the

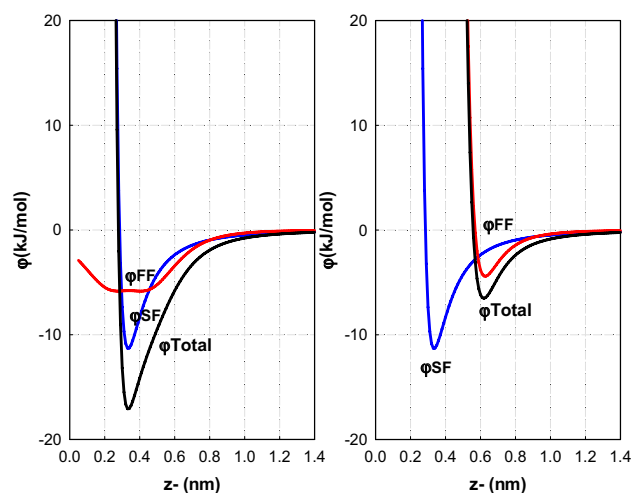


Fig. 9 The left panel shows the potential energies between one selected argon molecule in the monolayer with graphite (blue line) and the remaining molecules in the monolayer (red line) as it moves vertically away from the graphite surface. The right panel shows the potential energies between a molecule in the second layer with graphite (blue) and all molecules in the first layer (red). For both panels, the black line is the total potential energy

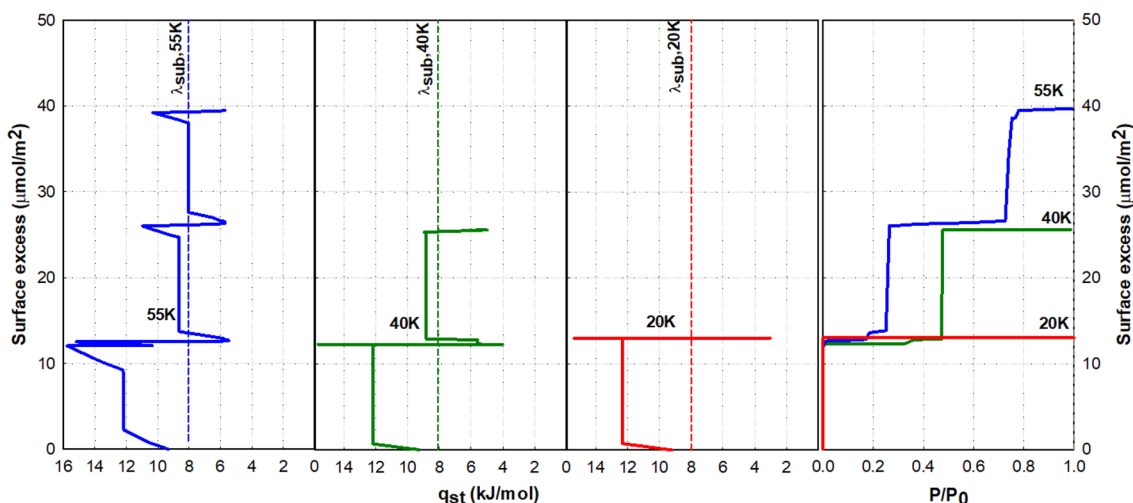


Fig. 8 Isothermic heats versus loading (left three panels) and isotherms versus the reduced pressure (right panel) for argon adsorption at 20 K, 40 K and 55 K on graphite. The vertical dashed lines are the heats of sublimation at these temperatures

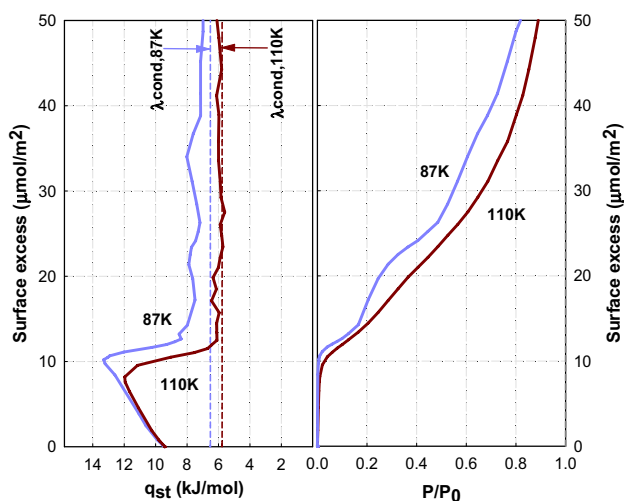


Fig. 10 Isosteric heats versus loading (left panel) and isotherms versus the reduced pressure for argon adsorption at 87 K and 110 K on graphite. The vertical dashed lines are the heats of evaporations at 87 K and 110 K

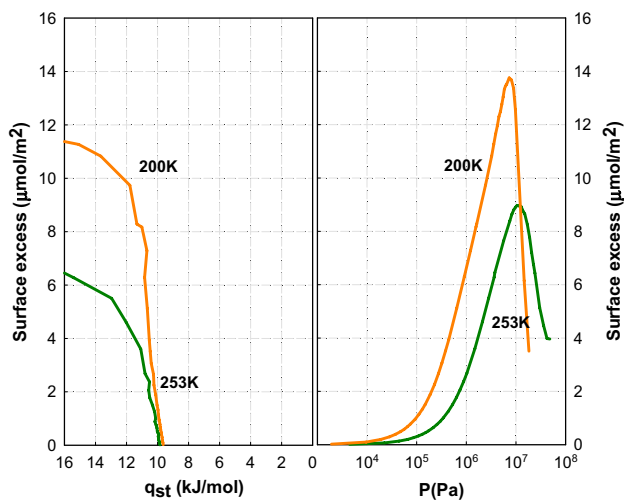


Fig. 11 Isosteric heats versus loading (left panel) and isotherms versus pressure (right panel) for argon adsorption at 200 K and 253 K on graphite

total energy of interaction, the blue line is the energy of this selected molecule with graphite, and the red line is the energy with the remaining molecules. The minimum of this potential energy is about 16.8 kJ/mol, which is very close to the maximum of 16 kJ/mol as seen in the isosteric heat versus loading (the small difference is due to the discrete calculations of the isosteric heat), confirming that the maximum in the heat curve at the monolayer density is the heat released when molecules enter the first layer to form regular hexagonal packing.

Beyond the maximum in the isosteric heat for 20 K, the heat decreases very sharply to 5 kJ/mol, which is less than

the heat sublimation of 8 kJ/mol (Fig. 8). This is the heat released by the first molecule coming on top the dense first layer. We substantiated this with a configuration of the dense first layer and a molecule adsorbing on this layer. Similarly, to what we did earlier, we moved this molecule vertically and calculated its energies of interactions with the surface and molecules in the first layer. This is shown in the right panel in Fig. 9, with the black line being the total energy of interaction and its contributions from the interactions between this molecule and the surface (blue line) and the molecules in the first layer (red line). The minimum is found to be 5 kJ/mol, which is in excellent agreement with the minimum in the plot of the isosteric heat versus loading, confirming that the minimum in the heat curve is the heat released when the first molecule adsorbs on the dense first layer. Since the heat of adsorption is less than the bulk heat of sublimation, spreading of molecules on the dense first layer is not favoured, but rather molecules added to the system would tend to form clusters, resulting in an increase in the interaction not only between molecules in these clusters but also between molecules in the clusters and those in the first layer. However, as the bulk coexistence pressure has been reached, the isosteric heat remains less than the bulk heat of sublimation, leading to the crossing between the adsorption isotherm and the P_0 axis and partial wetting of one layer is resulted for 20 K.

Let us now turn to the analysis of the isosteric heat versus loading at 40 K. Its pattern is similar to what was explained for 20 K for the first layer. As the first layer is completed, the isosteric heat decreases sharply to a minimum, resulting from the first molecule adsorbing on top of the first layer and the heat released is from its interaction with the three nearest neighbouring molecules in the first layer. The difference between this and the case of 20 K is that the isosteric heat due to the interactions among further molecules coming onto the top of the first layer is greater than the bulk heat of sublimation before the bulk coexistence pressure has been reached, resulting in the first-order condensation of the second layer (Fig. 8). This is so because the interface of the first layer for 40 K is more undulated that the adsorbate–adsorbate interactions are greater, compared to 20 K, and as a result, the heat released from these interactions makes the isosteric heat of adsorption greater than the heat of sublimation; hence the formation of the second layer, which occurs at a pressure less than the bulk coexistence pressure. As the pressure is further increased, the second layer is further densified as seen in the second maximum in the heat curve. Once this is completed, the isosteric heat is once again decreased to a second minimum, due to the incoming molecule on top of the dense second layer. Finally, as the pressure approaches the bulk coexistence pressure, the increase in the isosteric heat due to the interactions between adsorbed molecules

is not sufficient to induce the first-order transition of the third layer. This is the case of partial wetting with two layers. There are two interesting features on the evolution of the isosteric heat for the formation of the first and second layers. The peak in the isosteric heat when the first layer is completed is higher than the one for the second layer. This is because of the weaker interaction between molecules in the second layer and the solid. The second feature is the minima of the isosteric heat curve when the first molecule adsorbs onto the top of the first dense layer and onto the top of the second dense layer. If these dense layers are identical in structure, we would expect that the isosteric heats at these minima should be the same, but it is observed that the heat released for the first molecule adsorbing on top of the first layer is less than the heat when the first molecule adsorbing onto the top of the second layer. This is simply due to the greater undulation of the interface of the adsorbed film of two layers, resulting in better interaction between the incoming molecule and the neighbouring molecules in the second layer, compared to the case when the first molecule adsorbing onto the top of the better structured first layer. This is seen in the local density distribution in Fig. 5, where we see that the second layer is less organised, resulting in the greater interaction between the incoming molecule and the second layer.

The behaviour of the isosteric heat curve for 55 K shown in Fig. 8 is similar to what we explained for the case of 40 K.

- Temperatures between the bulk triple point and critical point temperatures

The isosteric heats of adsorption at 87 K and 110 K show different features to the ones seen for temperatures less than the bulk triple point temperature T_{Tr} (Fig. 10). Instead of the regular structure observed for temperatures less than T_{Tr} , the isosteric heat exhibits a monotonic increase with loading and reaches a maximum of 13.2 kJ/mol at the completion of the first layer. This is less than 16 kJ/mol observed for temperatures less than T_{Tr} , which is due to the high thermal fluctuations such that the inter-molecular spacing for 87 K and 110 K is larger than the optimal spacing of $2^{1/6}\sigma_{ff}$. Once the first layer is formed, the isosteric heat decreases due to the diminishing contribution from the adsorbate–adsorbent interactions in the formation of the second and higher layers, and it finally approaches the heat of condensation at high loadings.

- Temperatures above the bulk critical point temperature

The isosteric heats of adsorption for temperatures above the bulk critical point temperature are shown in Fig. 11. They exhibit an increase at low loadings, due to the

adsorbate–adsorbate interactions, and when the maximum in the excess density has been reached the isosteric heat becomes infinity, which is known as an artefact because the excess density is not amenable to the thermodynamic analysis. Absolute density must be considered in the calculation of the isosteric heat, for example, the absolute density of the adsorbed film [32] or the density of the whole system [34].

3.2 Weakly adsorbing solid

3.2.1 Adsorption isotherm

We now turn to the analysis of the argon adsorption on the weak substrate of $D^* = 3.5$. The wetting map in Fig. 1 indicates no wetting for temperatures below the wetting temperature of 100 K, which is specific for this weak substrate.

- Temperatures above the wetting temperature

We studied the isotherm for argon adsorption at 110 K on the weak substrate, as shown in Fig. 12. The figure also shows the 87 K and 110 K-isotherms for graphite for comparison. At low loadings, molecules form clusters on the surface of the weak surface (concave part of the isotherm), and it takes higher pressures for these clusters to merge to form adsorbed film and as the pressure approaches the bulk coexistence pressure the density tends to infinity, preceded by a pre-wetting of thin-to-thick transition, because 110 K falls in the region of pre-wetting for this weak substrate (Fig. 1).

- Temperatures above the bulk critical point temperature

The comparison between the adsorption isotherms for the weak surface and the graphite at temperatures above the critical point temperature is presented in Fig. 13 for 200 K and 253 K. The behaviour for the weak substrate is the same as that for graphite, with lower adsorbed density because of the weaker affinity of the substrate.

3.2.2 Local density distribution

- Temperatures between the bulk triple point and critical point temperatures

Figure 14 shows the comparison of the LDDs for argon adsorption at 110 K and P_0 on the weak substrate (continuous line) and graphite (dashed line). They both exhibit the complete wetting, and peaks for the weak substrate are lower, which is due to low interactions between the adsorbate and the weak substrate such that molecules do not pack efficiently on the surface, resulting in lower density of the first layer. As the loading is increased for both the weak substrate and graphite, the behaviour of the

Fig. 12 Isotherms for argon adsorption on graphite (dashed lines) and the weak surface (solid lines) at temperatures (87 K and 110 K) between the bulk triple point and critical temperatures

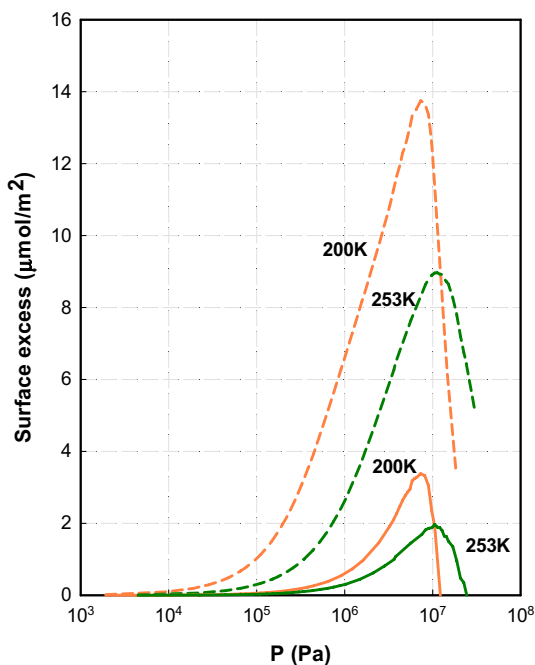
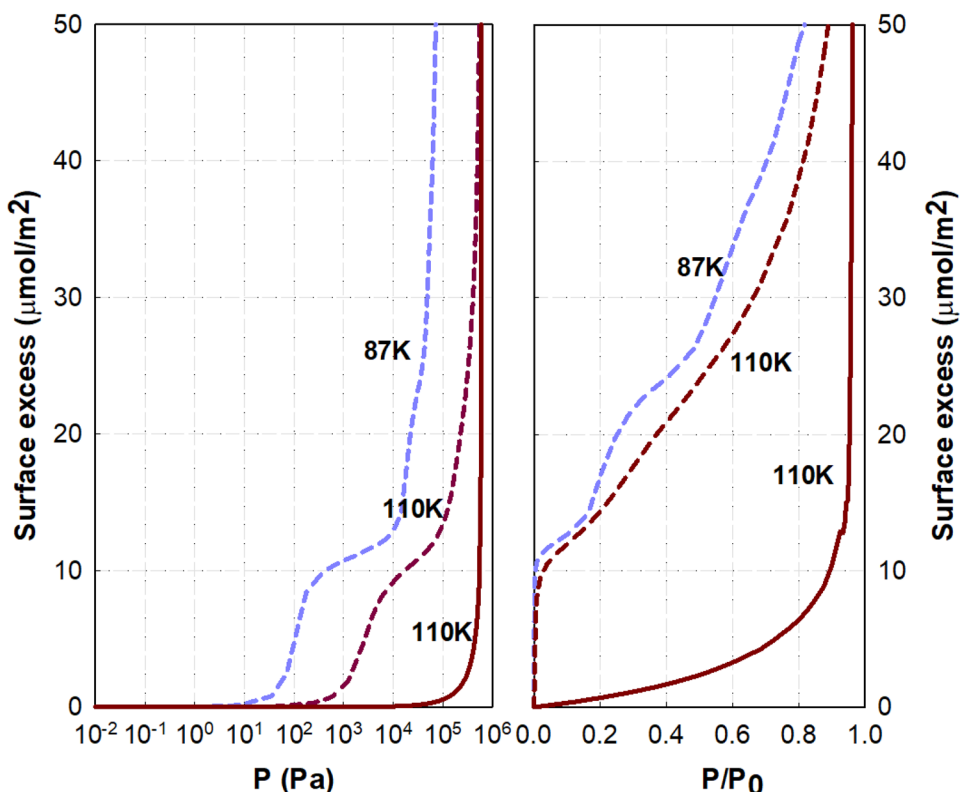


Fig. 13 Isotherms for argon adsorption on graphite (dashed lines) and the weak surface (solid lines) at temperatures above the bulk critical temperature

adsorbate far away from the surface is the same because of the diminishing contribution from the surface force. When the pressure approaches the bulk coexistence pressure, complete wetting occurs, purely due to the adsorbate–adsorbate interactions.

- Temperatures above the bulk critical point temperature

The LDDs for argon adsorption at 200 K on the strong and weak substrates are presented in Fig. 15. They both show an oscillating behaviour, and as discussed earlier, this does not mean that the excess density is greater than the statistical monolayer density because the peaks and troughs for second and higher layers cancel out (see yellow regions in the figure). The difference between the strong and weak substrates is that the magnitude of the LDD for the weak substrate is less than that for graphite, and its excess density is also less for a given pressure (Fig. 13).

3.2.3 Isosteric heat as a function of loading

- Temperatures above the wetting temperature

The comparison of the isosteric heat curves for argon adsorption on graphite and the weak substrate at 110 K is presented in Fig. 16, and we see the distinct difference

Fig. 14 Local density distributions (LDDs) for argon adsorption at 110 K on the weak surface at the coexistence pressure P_0 . The dashed line is the corresponding LDD for graphite shown for comparison

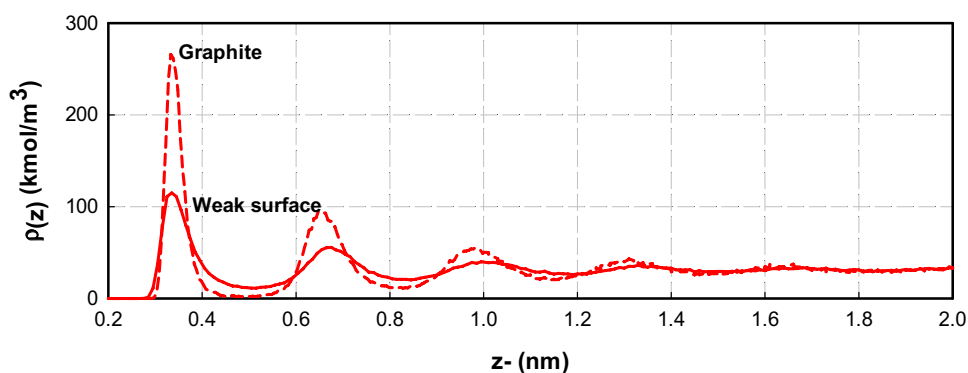


Fig. 15 Local density distributions (LDDs) for argon adsorption at 200 K and 1.62×10^7 Pa on the weak surface. The dashed line is the corresponding LDD for adsorption on graphite for comparison

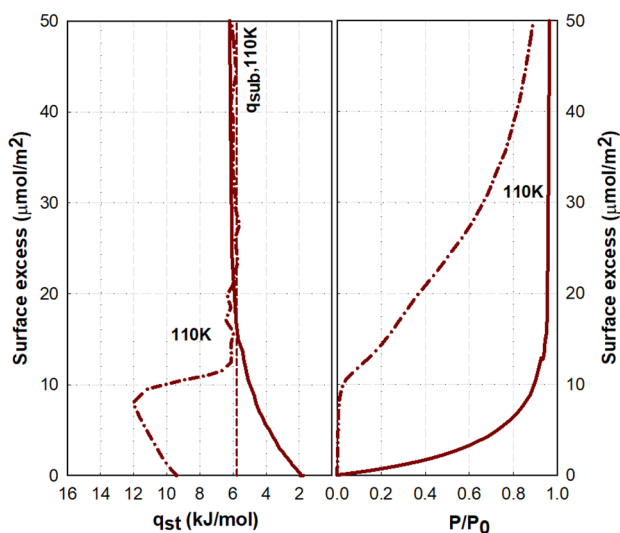
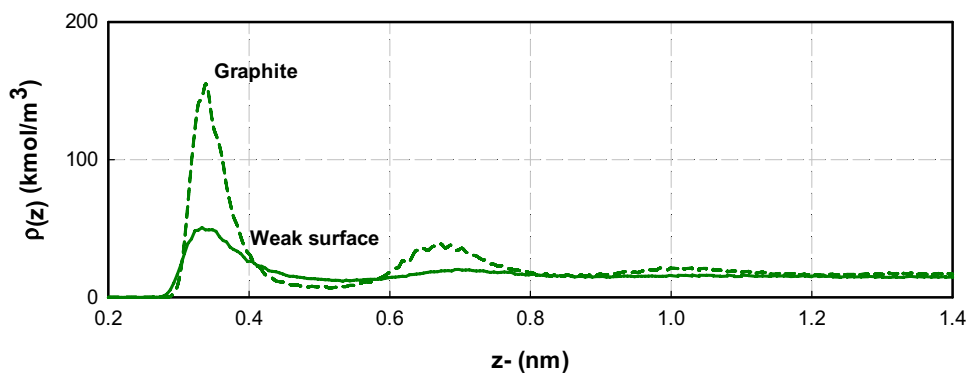


Fig. 16 Isosteric heats versus loading (left panel) and isotherms in terms of the reduced pressure (right panel) for argon adsorption at 110 K on graphite (dashed line) and the weak surface (solid line). The vertical dashed line is the heat of evaporation of bulk argon at 110 K

between these curves. For the weak substrate, the isosteric heat at zero loading is 2 kJ/mol, much lower than the heat of evaporation of 6 kJ/mol. This means that the interaction between argon molecule and the weak substrate

is not favoured, and therefore incoming molecules onto the surface tend to form clusters. When more molecules are added onto the surface with increasing pressure, the clusters increase in size and begin to merge to each other, resulting in greater adsorbate–adsorbate interactions; hence the isosteric heat increases up to a loading of $15 \mu\text{mol}/\text{m}^2$, at which the isosteric heat equals the heat of condensation. Therefore, a further increase in pressure leads to the formation of higher layers, and when the pressure approaches the bulk coexistence pressure, the adsorbed density tends to infinity, a complete wetting behaviour. The behaviour of the isosteric heat curve for the weak substrate corroborate the LDD that we discussed in the last section.

- Temperatures above the bulk critical point temperature

The isosteric heats of adsorption at temperatures above the critical point temperature are presented in Fig. 17, and they show the same behaviour as discussed earlier for graphite. Their approach to infinity at the maximum loading is known as the artefact because the excess isotherm is not amenable to thermodynamic analysis.

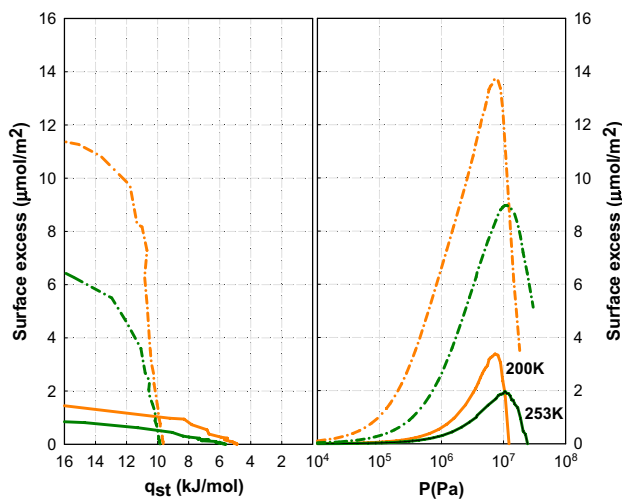


Fig. 17 Isosteric heats versus loading (left panel) and isotherms versus the pressure (right panel) for argon adsorption at temperatures above the bulk critical temperature on graphite (dashed line) and the weak surface (solid line)

4 Conclusions

We have presented the evolution of the simulated excess isotherm and the isosteric heat for argon adsorption on graphite, representing a strong adsorbing substrate, and a weak planar substrate over a wide range of temperatures, spanning from well below the triple point temperature to well above the critical point temperature of the bulk phase. Their evolution is also supported by the analysis of the local density distribution and the isosteric heat of adsorption versus loading. The adsorption behaviours show the change of the system from a state of either non-wetting or partial wetting to complete wetting as either the temperature or the surface strength is increased. The states of non-wetting and complete wetting are correlated with the difference between the isosteric heat of adsorption and the heat of sublimation (condensation) for temperatures below (above) the bulk triple point temperature; adsorption is favoured when the isosteric heat is greater than the heat of sublimation (condensation). For graphite, systems of argon adsorption at temperatures below the bulk triple point temperature exhibit the partial wetting at the bulk coexistence pressure, P_0 , at which the number of molecular layers depends on the temperature. The adsorbed density at P_0 is finite, and the isotherm cuts the P_0 axis at 90-degree angle because the isosteric heat remains less than the heat of sublimation. Another interesting feature in the analysis of isotherms for temperatures below the bulk triple point temperature is that the adsorbed density for the first layer is greater for lower temperatures at a given reduced pressure while for the second and higher layers (if existed) their densities is lower for lower temperatures at the same reduced pressure. This is due to the greater isosteric heat at

zero loading than the heat of sublimation for the first layer, and the lower isosteric heat than the heat of sublimation at the onset of the second and higher layers. For temperatures greater than the bulk triple point temperature, but below the bulk critical temperature, argon/graphite system exhibits a complete wetting at P_0 because the isosteric heat is greater than the heat of condensation, resulted from the highly undulated interface between the adsorbed phase and the bulk gas surrounding, and the adsorbed density is greater for lower temperature at a given reduced pressure because the isosteric heat is always greater than the heat of condensation.

For systems of argon/weak substrate, non-wetting occurs for temperatures below the wetting temperature because of the lower isosteric heat than the heat of sublimation and the adsorbed density at P_0 is much less than the statistical monolayer density. Only when the temperature is increased above the wetting temperature, the system exhibits complete wetting, and finally when the temperature is above the bulk critical temperature the excess density exhibits a maximum, but the loading is much less than that for strongly adsorbing graphite because of the weak surface force which is not enough to densify the adsorbate near the surface.

Acknowledgements This project is supported by the Australian Research Council (DP160103540).


References

- Robens, E., Jayaweera, S.A.A.: Early history of adsorption measurements. *Adsorption*. **32**(6), 425–442 (2014). <https://doi.org/10.1260/0263-6174.32.6.425>
- Gatica, S.M., Cole, M.W.: To wet or not to wet: that is the question. *J. Low Temp. Phys.* **157**(3–4), 111–136 (2009). <https://doi.org/10.1007/s10909-009-9885-z>
- Schlangen, L.J.M.: *Adsorption and wetting: experiments, thermodynamics and molecular aspects*. Schlangen, S.I (1995). Retrieved from <https://edepot.wur.nl/205414>
- Steele, W.A.: Wetting phenomena. In: Eduardo, J.B., Juan, M.D.T. (eds.) *Adsorption by Carbons*, pp. 167–185. Elsevier, Amsterdam (2008)
- Ahmad, D., van den Boogaert, I., Miller, J., Presswell, R., Jouhara, H.: Hydrophilic and hydrophobic materials and their applications. *Energy Source A* **40**(22), 2686–2725 (2018). <https://doi.org/10.1080/15567036.2018.1511642>
- Erfani Gahrooei, H.R., Ghazanfari, M.H.: Application of a water based nanofluid for wettability alteration of sandstone reservoir rocks to preferentially gas wetting condition. *J. Mol. Liq.* **232**, 351–360 (2017). <https://doi.org/10.1016/j.molliq.2017.02.097>
- Wang, Z., Elimelech, M., Lin, S.: Environmental applications of interfacial materials with special wettability. *Environ. Sci. Technol.* **50**(5), 2132–2150 (2016). <https://doi.org/10.1021/acs.est.5b04351>
- Yin, Y., Hang, L., Xu, J., McKenzie, D.R., Bilek, M.M.M.: Surface adsorption and wetting properties of amorphous diamond-like carbon thin films for biomedical applications. *Thin Solid Films.* **516**(16), 5157–5161 (2008). <https://doi.org/10.1016/j.tsf.2007.07.012>

9. Loi, Q.K., Prasetyo, L., Tan, S., Do, D.D., Nicholson, D.: Nonwetting/prewetting/wetting transition of ammonia on graphite. *Langmuir* **35**(3), 641–652 (2019). <https://doi.org/10.1021/acs.langmuir.8b03634>
10. Prasetyo, L., Loi, Q.K., Tan, S.J., Do, D.D., Nicholson, D.: Effects of temperature on the transition from clustering to layering for argon adsorption on substrates of different strength: parametric map of wetting, pre-wetting and non-wetting. *Microporous Mesoporous Mater.* (2018). <https://doi.org/10.1016/j.micromeso.2018a.12.023>
11. Prasetyo, L., Xu, H., Fan, C., Do, D.D., Nicholson, D.: On the coexistence pressure between the bulk and adsorbed argon on substrates of different strength: temperature dependence of the characteristics of the adsorbate. *Chem. Eng. J.* **378**, 122214 (2019). <https://doi.org/10.1016/j.cej.2019.122214>
12. Xu, H., Zeng, Y., Do, D.D., Nicholson, D.: On the nonwetting/wetting behavior of carbon dioxide on graphite. *J. Phys. Chem. C* **123**(14), 9112–9120 (2019). <https://doi.org/10.1021/acs.jpcc.9b00635>
13. Dunne, J.A., Mariwala, R., Rao, M., Sircar, S., Gorte, R.J., Myers, A.L.: Calorimetric heats of adsorption and adsorption isotherms. 1. O₂, N₂, Ar, CO₂, CH₄, C₂H₆, and SF₆ on silicalite. *Langmuir* **12**(24), 5888–5895 (1996). <https://doi.org/10.1021/la960495z>
14. Sircar, S.: Gibbsian surface excess for gas adsorption revisited. *Ind. Eng. Chem. Res.* **38**(10), 3670–3682 (1999). <https://doi.org/10.1021/ie9900871>
15. Sircar, S.: Measurement of gibbsian surface excess. *AIChE* **47**(5), 1169–1176 (2001)
16. Sircar, S., Cao, D.V.: Heat of adsorption. *Chem. Eng. Technol.* **25**(10), 945–948 (2002)
17. Sircar, S., Mohr, R., Ristic, C., Rao, M.B.: Isotheric heat of adsorption: theory and experiment. *J. Phys. Chem. B* **103**(31), 6539–6546 (1999). <https://doi.org/10.1021/jp9903817>
18. Sircar, S., Rao, M.B.: Heat of adsorption of pure gas and multi-component gas mixtures on microporous adsorbents. In: Schwarz, J.A., Contescu, C.I. (eds.) *Surface of Nanoparticles and Porous Materials*, pp. 501–528. Marcel Dekker Inc, New York (1999)
19. Prasetyo, L., Tan, S., Akram, A., Do, D.D., Nicholson, D.: Cluster growth and coalescence of argon on weakly adsorbing substrates: the origin of the thin-to-thick film transition. *Colloids Surf. A* **554**, 169–179 (2018). <https://doi.org/10.1016/j.colsurfa.2018.06.037>
20. Nguyen, V.T., Do, D.D., Nicholson, D.: Monte Carlo simulation of the gas-phase volumetric adsorption system: effects of dosing volume size, incremental dosing amount, pore shape and size, and temperature. *J. Phys. Chem. B* **115**(24), 7862–7871 (2011). <https://doi.org/10.1021/jp202073r>
21. Nguyen, V.T., Do, D.D., Nicholson, D.: Reconciliation of different simulation methods in the determination of the equilibrium branch for adsorption in pores. *Mol. Simul.* **40**(7–9), 713–720 (2014). <https://doi.org/10.1080/08927022.2013.829229>
22. Johnson, J.K., Zollweg, J.A., Gubbins, K.E.: The Lennard-Jones equation of state revisited. *Mol. Phys.* **78**(3), 591–618 (1993)
23. Michels, A., Wijker, H., Wijker, H.: Isotherms of argon between 0°C and 150°C and pressures up to 2900 atmospheres. *Physica* **15**(7), 627–633 (1949). [https://doi.org/10.1016/0031-8914\(49\)90119-6](https://doi.org/10.1016/0031-8914(49)90119-6)
24. Steele, W.A.: The physical interaction of gases with crystalline solids: I Gas-solid energies and properties of isolated adsorbed atoms. *Surf. Sci.* **36**(1), 317–352 (1973)
25. Herrera, L.F., Prasetyo, L., Do, D.D.: Characterisation of the absolute accessible volume of porous materials. *Adsorption* (2019). <https://doi.org/10.1007/s10450-019-00078-6>
26. Chen, B., Siepmann, J.I., Klein, M.L.: Direct Gibbs ensemble Monte Carlo simulations for solid-vapor phase equilibria: applications to Lennard-Jonesium and carbon dioxide. *J. Phys. Chem. B* **105**(40), 9840–9848 (2001). <https://doi.org/10.1021/jp011950p>
27. Tan, S.J., Prasetyo, L., Zeng, Y., Do, D.D., Nicholson, D.C.: On the consistency of NVT, NPT, μ VT and Gibbs ensembles in the framework of kinetic Monte Carlo: fluid phase equilibria and adsorption of pure component systems. *Chem. Eng. J.* **316**, 243–254 (2017)
28. Do, D.D., Do, H.D., Nicholson, D.: Molecular simulation of excess isotherm and excess enthalpy change in gas-phase adsorption. *J. Phys. Chem. B* **113**(4), 1030–1040 (2009). <https://doi.org/10.1021/jp8046467>
29. Rouquerol, J., Rouquerol, F., Llewellyn, P., Denoyel, R.: Surface excess amounts in high-pressure gas adsorption: issues and benefits. *Colloids Surf. A* **496**, 3–12 (2016). <https://doi.org/10.1016/j.colsurfa.2015.10.045>
30. Do, D.D., Do, H.D.: Adsorption of argon from sub- to supercritical conditions on graphitised thermal carbon black and in graphitic slit pores: a grand canonical Monte Carlo simulation study. *J. Chem. Phys.* **123**(8), 211 (2005)
31. Do, D.D., Do, H.D., Fan, C.Y., Nicholson, D.: On the existence of negative excess isotherms for argon adsorption on graphite surfaces and in graphitic pores under supercritical conditions at pressures up to 10,000 atm. *Langmuir* **26**(7), 4796–4806 (2010)
32. Phadungbut, P., Fan, C., Do, D.D., Nicholson, D., Tangsathitkulchai, C.: Determination of absolute adsorption for argon on flat surfaces under sub- and supercritical conditions. *Colloids Surf. A* **480**, 19–27 (2015). <https://doi.org/10.1016/j.colsurfa.2015.04.011>
33. Zeng, Y., Xu, H., Do, D.D., Nicholson, D.: Adsorption of argon on graphitised carbon black preloaded with methanol, ammonia and water: the role of adsorption regions and adsorbates. *Chem. Eng. J.* **334**, 1316–1327 (2018). <https://doi.org/10.1016/j.cej.2017.11.098>
34. Xu, H., Prasetyo, L., Do, D.D., Nicholson, D.: The Henry constant and isotheric heat at zero loading for adsorption on energetically heterogeneous solids absolute versus excess. *Chem. Eng. J.* **395**, 125035 (2020). <https://doi.org/10.1016/j.cej.2020.125035>

Publisher's note Springer Nature remains neutral with regard to jurisdictional claims in published maps and institutional affiliations.

Authors and Affiliations

Luis Herrera¹ · Quang K. Loi² · Luisa Prasetyo² · D. D. Do² 

✉ D. D. Do
d.d.do@uq.edu.au

¹ College of Engineering, IT and Environment, Charles Darwin University, Darwin, NT 0909, Australia

² School of Chemical Engineering, University of Queensland, St. Lucia, QLD 4072, Australia